Journal of Geography and Geology; Vol. 16, No. 1; 2024
ISSN 1916-9779 E-ISSN 1916-9787
Published by Canadian Center of Science and Education

Connection between El Niño Deep Convection and Precipitation in Northeast Brazil

Isimar Santos[1]

[1] Retired, Rio de Janeiro, Brazil

Correspondence: Isimar Santos, Retired, Rio de Janeiro, Brazil. Mobile: 55-21-992489293. E-mail: isimarsantos@gmail.com

Received: December 23, 2023 Accepted: January 21, 2024 Online Published: January 23, 2024

doi: 10.5539/jgg.v16n1p17 URL: https://doi.org/10.5539/jgg.v16n1p17

Abstract

The indices reflecting the warm or cold phases of the El Niño-Southern Oscillation (ENSO) phenomenon are commonly based on sea surface temperature (SST) anomalies in cleverly chosen sectors in the Tropical Pacific Ocean. These climate indices, used as predictors of remote climate oscillations, have been successful in most studies of the effects of ENSO forcings on drought anomalies or unexpected floods worldwide. However, there is one difficulty that bothers researchers: the diversity of these remote effects. One of the regions of the world that has attracted the attention of scholars of the remote effects of ENSO oscillations is Northeast Brazil. The main reason for this interest is the great vulnerability of this region to droughts due to the social and economic fragilities that have persisted there for more than two centuries. This study proposes the experimental use of atmospheric indices, such as convective instability, as indicators of the presence of cumulonimbus in the Tropical Pacific in response to El Niño episodes. It is well known that the remote effects of El Niño events occur due to cumulonimbus formation in the Tropical Pacific in response to the additional supply of heat and humidity in areas with warm surface waters. However, these tropical cumulus clusters respond not only to surface heating but also to other forces associated with atmospheric circulation. This study has shown that such cumulonimbi can form in areas that are slightly apart from the sectors with the greatest surface heating.

Keywords: convective instability, drought in Northeast Brazil, El Niño-Southern Oscillation

1. Introduction

Field investigations analyzed by Sir Gilbert Walker in the early decades of the 20th century indicated that there was a significant connection between some special atmospheric conditions in the Tropical Pacific Ocean and episodes of drought or anomalously intense rainfall in various locations around the world. Walker and Bliss (1932) published the results of an analysis of time series of rainfall data collected in Fortaleza, Brazil, confirming the existence of connections between periods of drought in Northeast Brazil (NEB) and a seesaw of atmospheric pressure between Tahiti, in the central tropical Pacific, and Darwin, on the northern Australian coast. Walker called this phenomenon the Southern Oscillation. Subsequent studies have shown that there is a marked coincidence between the Southern Oscillation and the anomalous increase in sea surface temperature (SST) in the Tropical Pacific Ocean, a phenomenon that strongly affects fishing activity off the Peruvian coast. Today, climatologists understand that two phenomena, the atmospheric phenomenon of the Southern Oscillation and the anomalous warming of the tropical waters of the Eastern and Central Pacific, are physically associated (Katz, 2002).

Droughts have been occurring on the planet for a long time, and in recent years, their frequency and intensity have increased, mainly in response to population growth in regions with low productive capacity. Drought is undoubtedly the most impactful climatic phenomenon that occurs in the NEB region, causing countless social problems to accumulate throughout the history of this region, with the devastating drop in agricultural production being the main climatic risk. For more than a hundred years, the serious economic and social impacts related to drought events that affect the population of NEB have amply justified research into the climatic processes that are linked to drought in this region. Several studies have shown that drought in NEB, as an event of multiple proportions, has a risk aggravated due to preexisting conditions of economic and social vulnerabilities in the region (Hastenrath, 2012).

An enormous difficulty in studying the global effects triggered by the anomalous and occasional warming of the waters of the Tropical Pacific, the so-called El Niño, is the diversity in the characteristics of these remote effects, including their intensity and location. Reboita and Santos (2014) analyzed the diversity of responses to the occurrence of the warm phase of ENSO (El Niño-Southern Oscillation) on precipitation in NEB, also considering the influence of SST patterns in the Tropical Atlantic. Capotondi et al. (2015) address in depth and competently the issue of the diversity of the effects of the occurrence of the warm phase of ENSO, showing some of these effects in the form of teleconnections that affect the climate in the continental part of the United States of America. Chiodi and Harrison (2015) propose the use of satellite observations of outgoing longwave radiation over the Tropical Pacific as an alternative approach to identifying the physical processes triggering vertical circulation cells in response to El Niño surface warming.

The pioneering work of Yanai, Esbensen & Chu (1973) paved the way for various studies on the large-scale convective response to surface heating in the tropical atmosphere. Following this approach, Betts and Silva Dias (1979) showed that the vertical gradient of the equivalent potential temperature (θ_e) in the tropical lower troposphere is an excellent indicator of the presence of cumulonimbus in areas with surface heating. Silva Dias, Schubert & DeMaria (1983) also compared theoretical results with observed data in Tropical South America to elucidate how the tropical atmosphere responds to surface heating with intense deep convection.

The connection between the anomalous warming of tropical Pacific waters and drought episodes in various parts of the world occurs through the activation of vertical circulation cells, mainly Walker cells, which are driven by the deep convection that occurs naturally over warmer waters during El Niño episodes. From Walker's first propositions in the 1920s and 1930s until the 1960s, the most relevant studies of the Southern Oscillation and its possible teleconnections were carried out using atmospheric measurements, mainly pressure.

Although research into the climatic effects of the ENSO phenomenon has been carried out basically considering SST anomalies in the Tropical Pacific in recent decades, this study returns to the essentially atmospheric approach to diagnosing El Niño conditions, starting from the premise that it is not exactly the anomalous warming of Tropical Pacific waters that triggers vertical circulation cells in the atmosphere but rather the occurrence of deep cumulonimbus in response to such surface warming. It is important to bear in mind that the spatial distribution of these cumulonimbi is largely controlled by atmospheric forcings other than just the warming of seawater at the surface.

2. Methods

Since this study is essentially observational, we used sea surface temperature (SST) data and air temperature (T) and specific humidity (q_s) data at isobaric levels in the lower troposphere, as well as precipitation data. The sources of these data were the ERA-5 reanalysis products processed by the European Centre for Medium-Range Weather Forecasts (ECMWF) and obtained from the website cds.climate.copernicus.eu (Hersbach et al., 2023).

The following formulas are presented by Holton (2004, pp. 50 and 291) for calculating the potential temperature (θ) and the equivalent potential temperature (θ_e) and were used in this study. The environmental variables used in these formulations are explained in didactic texts such as the one just cited.

$$\theta = T\left(\frac{p_s}{p}\right)^{\frac{R}{c_p}} \quad (1)$$

$$\theta_e \approx \theta \exp\frac{L_c q_s}{c_p T} \quad (2)$$

In Figure 1, Yanai et al. (1973) present typical vertical profiles of the tropical atmosphere, as observed in an oceanic experiment using five radiosonde stations in the region of Bikini Island in the Tropical Pacific. The middle curve is the static moist energy profile ($\tilde{h}$).

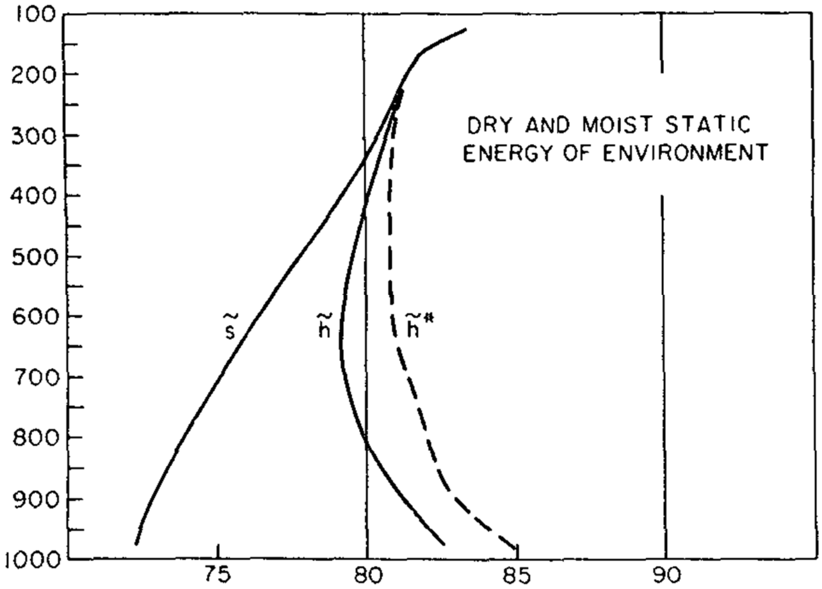

Figure 1. Vertical profiles in a typical tropical environment presented by Yanai et al. (1973) and referring to a field experiment

According to Holton (2004, p. 291), there exists proportionality between the vertical profile of moist static energy ($\tilde{h}$) proposed in Yanai et al. (1973) and the vertical profiles of the equivalent potential temperature (θ_e) of Equation (2). In this way, and looking at the inclination of the curves of θ_e below 700 hPa, Figure 2a represents examples of a stable tropical environment, while Figure 2b exemplifies an unstable tropical atmosphere.

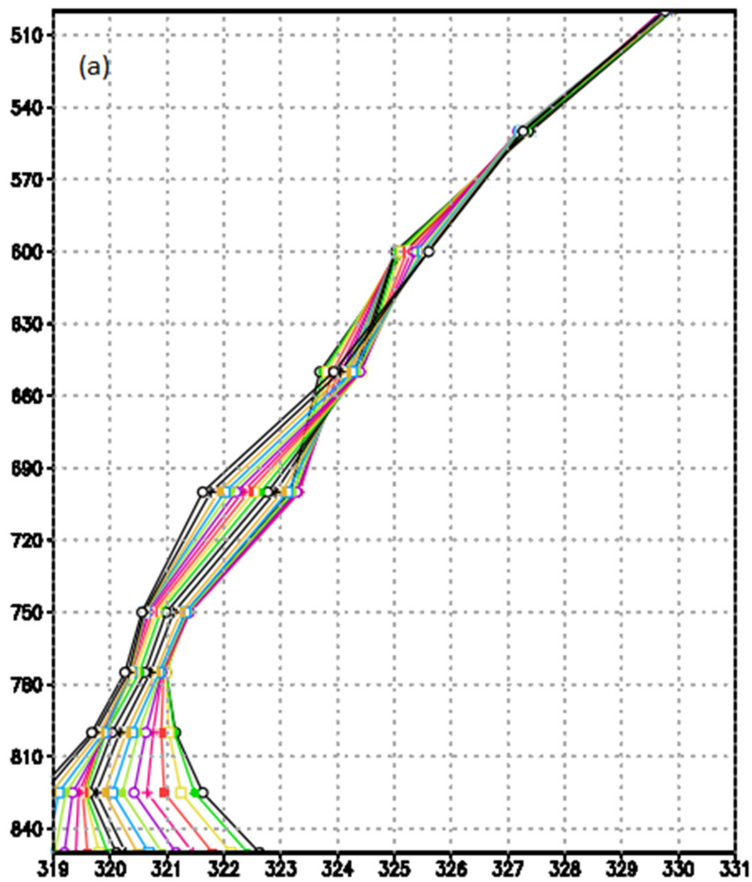

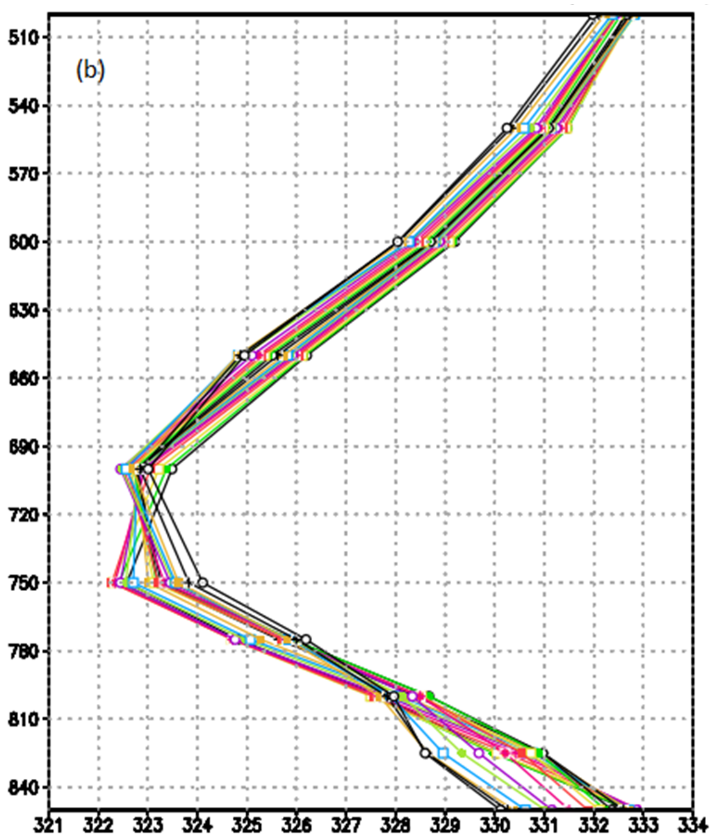

Figure 2. Vertical profiles of the equivalent potential temperature (θ_e) in the lower troposphere: (a) case of strong regional stability; (b) case of strong regional convective instability

Source of data: ERA-5 Reanalyzes of ECMWF.

These examples in Figure 2 suggest that the "gradients" of θ_e between 850 and 700 hPa are good indicators of the degree of atmospheric stability/instability, identifying the presence or absence of deep cumulus convection. Therefore, to obtain indications of convectively unstable atmospheric conditions in the sector of the Tropical Pacific where the upward arms of the vertical circulation cells occur in response to El Niño episodes, we used the temperature (T) and specific humidity (q_s) data obtained from the ECMWF ERA-5 reanalysis and calculated the "gradient" of θ_e between the isobaric levels of 850 and 700 hPa ($\Delta\theta_e/\Delta p$) at each grid point.

$$\boldsymbol{\nabla}(\theta_e) = \frac{\theta_e^{850} - \theta_e^{700}}{(850-700)\text{hPa}} \tag{3}$$

The conditions represented by the numerator of (3) should be positive for convectively unstable environments, i.e., environments with many cumulonimbi, while negative numerators indicate stable conditions.

To study the spatial and temporal distributions of rainfall in NEB and its possible connection with warm episodes of the El Niño-Southern Oscillation (ENSO) phenomenon, rainfall data from the ECMWF ERA5 reanalysis for the years 1980 to 2022 were used. Based on observational studies of rainfall in NEB (e.g., Kousky, 1980), in this study, this region was subdivided into 4 boxes that characterize different rainfall climatological behaviors (Figure 3).

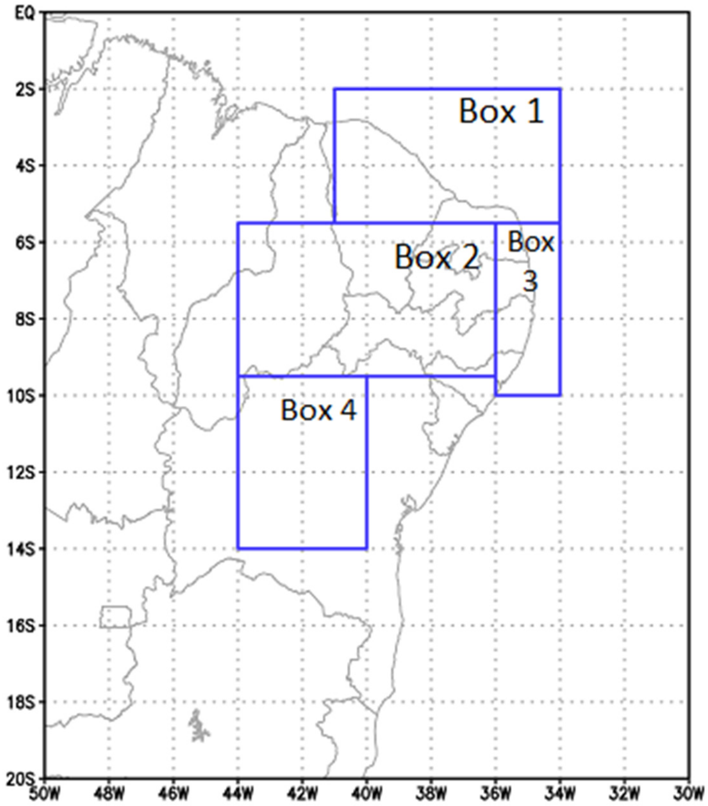

Figure 3. Subregions of Northeast Brazil for rainfall analysis: Box 1 – Northern Sector of NEB, Box 2 - Interior of NEB, Box 3 - Eastern Sector of NEB, Box 4 - Interior of the State of Bahia

In Figure 3, Box 1 corresponds to the northern sector of NEB, including the typical location of the western sector of the Atlantic Intertropical Convergence Zone (ITCZ) during the summer and fall of the Southern Hemisphere, directly affecting rainfall in this sector of the Atlantic ITCZ; Box 2, corresponding to the interior of NEB, is the region that suffers most from prolonged droughts due to its enormous social and economic vulnerability; Box 3 is the Eastern Sector of NEB, a region little affected by droughts because it receives coastal moisture and is therefore reasonably well served by rainfall; and Box 4, corresponding to the interior of the State of Bahia in Brazil, is part of NEB but has a different rainfall regime, as will be seen below.

The composites used in this study were obtained through weighted averages of climatic variables such as precipitation in NEB or the vertical gradient of the equivalent potential temperature in the lower troposphere ($\Delta\theta_e/\Delta p$) in the Tropical Pacific over time. The weighting factors are climate indices, such as the Niño3.4 SST anomalies (Reboita & Santos, 2014).

3. Results and Discussion

The aim of this study was to determine the presence and spatial distribution of deep convection in the tropical sector of the Pacific Ocean in response to surface warming and greater availability of water vapor during El Niño events. This convection is represented here by the vertical gradient of the equivalent potential temperature ($\Delta\theta_e/\Delta p$).

3.1 Statistical Correlation between ENSO Events and Rainfall in Northeast Brazil

Using data from the ECMWF ERA-5 reanalysis, Figure 4 shows the spatial distribution, in the Tropical Pacific, of the correlations between the time series (for 43 years) of monthly SST anomalies at each grid point and the time series of monthly rainfall anomalies in Box 1, positioned in the northern strip of the NEB.

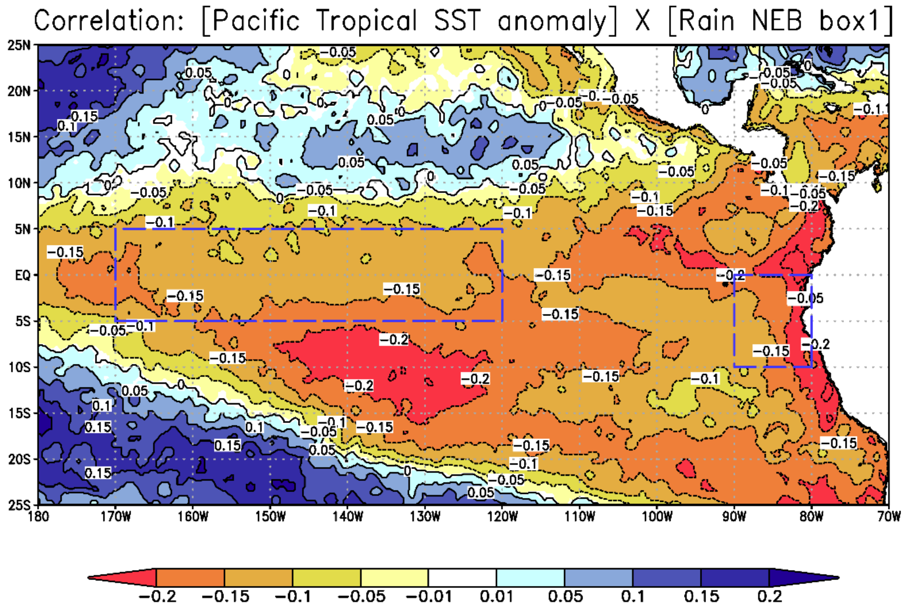

Figure 4. Regional distribution of the correlation between Tropical Pacific SST anomalies and rainfall anomalies in Box 1 of NEB. The Niño1+2 and Niño3.4 sectors are highlighted

Figure 4 shows good spatial consistency of the negative correlations observed over a large area of the Tropical Pacific, albeit with very low values, since they involve averages of correlations over 43 years. It is also noteworthy that the sector with the most significant values (average correlations of less than -0.2) appears south of the sector corresponding to Niño3.4, while to the north of this sector, there is an area with positive correlations, i.e., an area in which high values of positive SST anomalies are not connected to droughts in the north of NEB, at least during the period studied.

Figure 5 shows the spatial distribution of the correlations between the time series (43 years) of the monthly mean convection indices (the vertical gradient of θ_e in the lower troposphere) and the time series of monthly rainfall anomalies in Box 1 of NEB. The convective profiles were calculated at each grid point of the ECMWF ERA-5 reanalysis data.

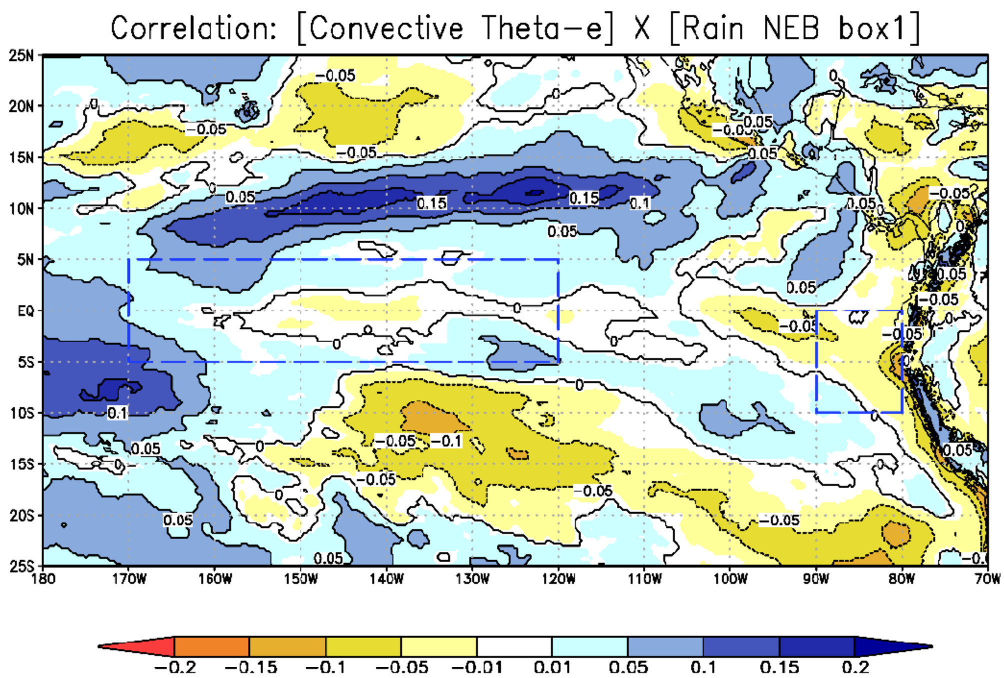

ui

Figure 5. Regional distribution of the correlation between the convective profiles point by point against precipitation anomalies in Box 1 of NEB. The Niño1+2 and Niño3.4 sectors are highlighted

Figure 5 shows that the rainfall anomalies north of NEB (Box 1) are very weakly associated with the Niño3.4 region, with a greater correlation with the sector to the south of this region but no physically coherent relationship with the sector to the north.

Figure 6 shows the spatial distribution of the correlations between the monthly SST anomalies in the Tropical Pacific and the time series of monthly rainfall anomalies in Box 2 within NEB. This time, the slightly more correlated area coincides with the Niño3.4 sector.

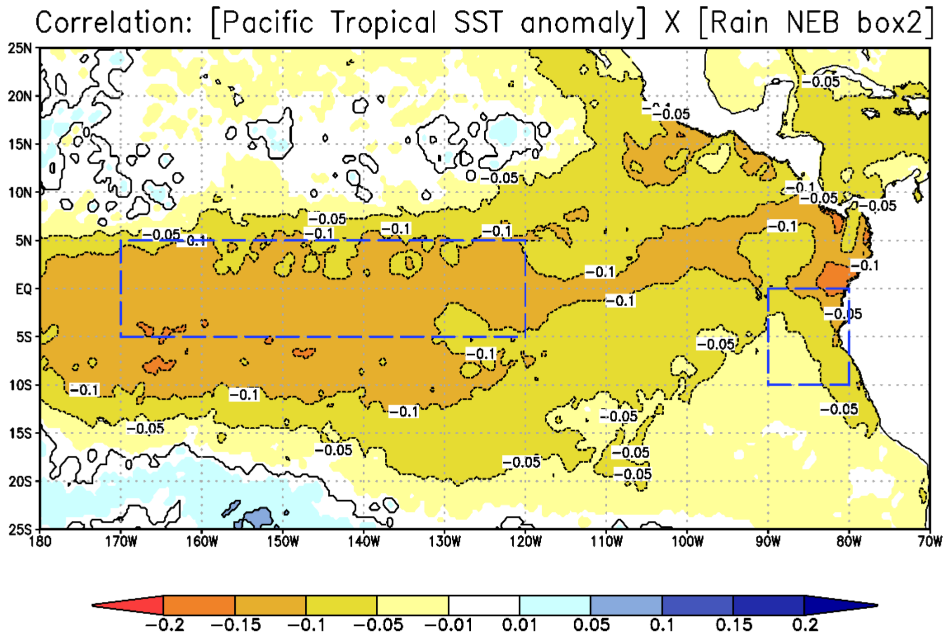

Figure 6. As in Figure 4 but referring to Box 2 of the NEB. The Niño1+2 and Niño3.4 sectors are highlighted

Figure 7 shows, in average values over time, the correlation between the presence of convection in the Tropical Pacific and the rainfall in Box 2 of NEB.

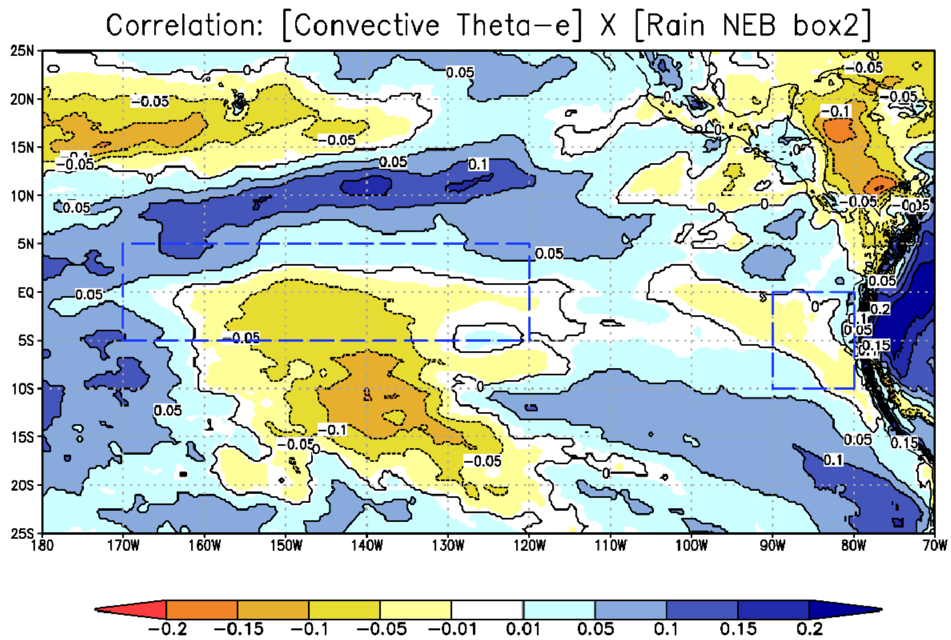

Figure 7. As in Figure 5 but referring to Box 2 of the NEB. The Niño1+2 and Niño3.4 sectors are highlighted

Figure 7 shows that a consistent area south of the Niño3.4 sector seems to have a greater affinity with the rainfall variations in Box 2 of NEB. On the other hand, Figure 7 indicates that there is no correlation between rainfall in the interior of Northeast Brazil and in the oceanic region to the north of the Niño3.4 sector. It is important to note that the Box 2 region in Northeast Brazil is the region that suffers most when long droughts occur, as it is very vulnerable socially and economically.

The spatial distribution of correlations between rainfall in NEB Box 3 and El Niño convection in the Tropical Pacific was obtained in this study but is not shown here. As previously stated, rainfall in Box 3 of NEB is favored by the good contribution of moisture inputs offered by the Tropical Atlantic Ocean and is little affected by remote influences such as ENSO oscillations.

Figure 8 shows the weak correlation between SST anomalies in the Tropical Pacific and rainfall in Box 4 of NEB.

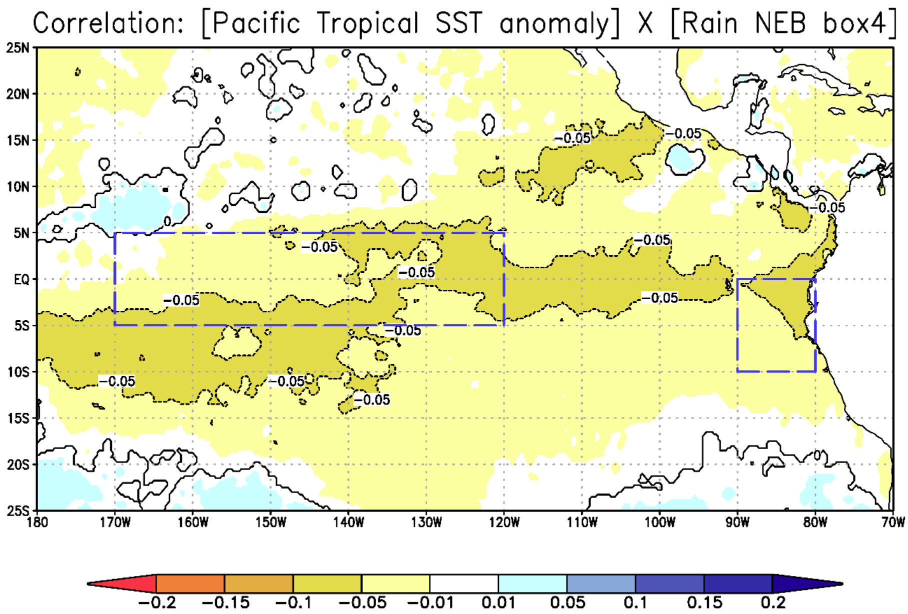

Figure 8. As in Figure 4 but referring to Box 4 of the NEB. The Niño1+2 and Niño3.4 sectors are highlighted

Figure 9 shows the correlations between the gradients $\Delta\theta_e/\Delta p$ observed at each grid point in the Tropical Pacific and the rainfall in Box 4 of NEB.

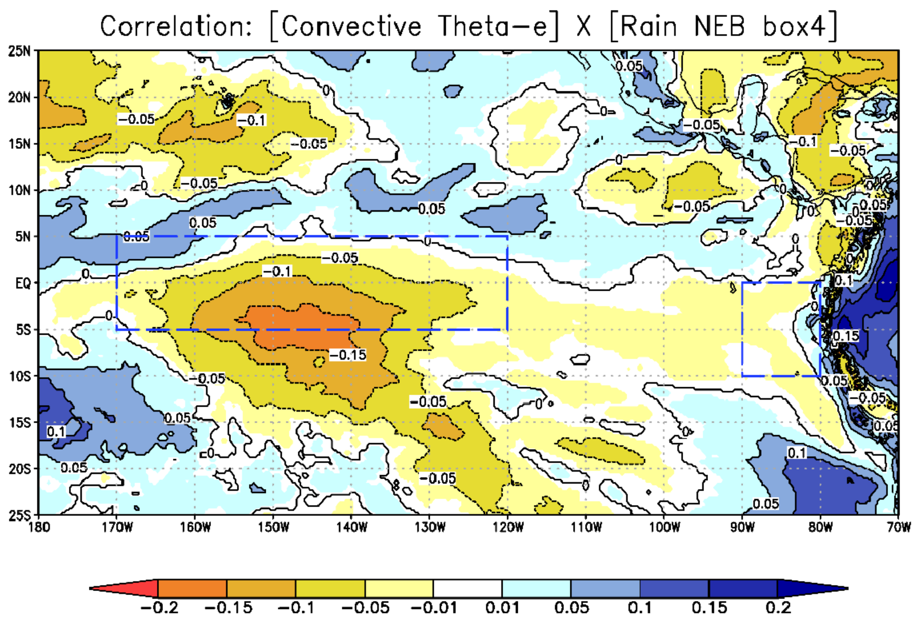

Figure 9. As in Figure 5 but referring to Box 4 of the NEB. The Niño1+2 and Niño3.4 sectors are highlighted

In Figure 9, the droughts that occur in the interior of the state of Bahia in Brazil (Box 4 of Figure 3) seem to be relatively well correlated with the warm water sector called Niño3.4 and to the south of it.

These results thus far show that although the correlations between rainfall and droughts in NEB seem to respond to the SST anomalies in the Niño3.4 sector, NEB's response to the forcing of the subsidence sector of the Walker cells during El Niño episodes arises at few degrees of latitude to the south.

3.2 Convective Response to Three Notable El Niño Episodes

Next, several diagnoses are presented for three notable El Niño episodes, namely, the 1982/1983 event, the 1997/1998 event and the most recent 2014/2015/2016 event. Once again, the convective response is investigated here through the spatial and temporal distributions of the vertical gradient θ_e between the isobaric levels 850 and 700 hPa ($\Delta\theta_e/\Delta p$) across the Tropical Pacific.

Figure 10 represents the convective response to the 1982/1983 El Niño observed in the Tropical Pacific through the composite of the gradients $\Delta\theta_e/\Delta p$ point-to-point. In the months from August 1982 to June 1983, the convective gradients were weighted using the average monthly SST anomalies of the Niño3.4 sector.

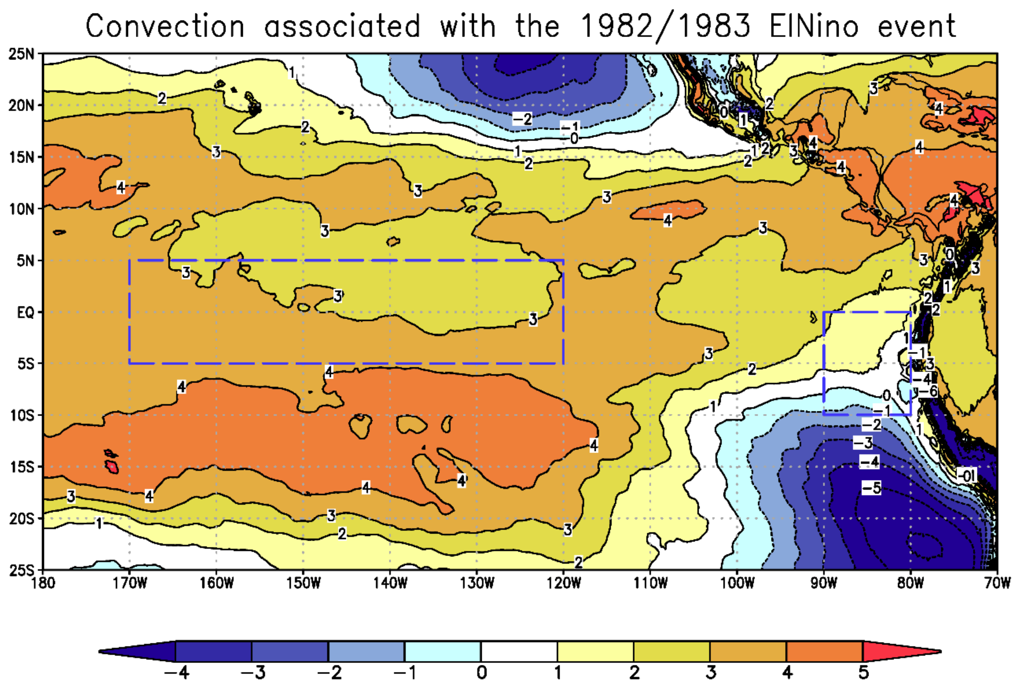

Figure 10. A composite representing the convective response to anomalous warming occurred during the El Niño event of 1982/1983. The Niño1+2 and Niño3.4 sectors are highlighted

Unit: 10^{-4} K/Pa

Considering that the vertical gradient of θ_e is positive for convectively unstable environments and negative for cold or stable environments, Figure 10 shows that the regions where convection was most effective during this warm event were south of the oceanic area related to the Niño 3.4 index.

Next, Figures 11 and 12 show the regional distributions of the monthly precipitation anomalies in Northeast Brazil in December 1982, when the monthly SST anomaly in the Niño 3.4 sector of the Pacific reached 2.20°C, and in January 1983, when the Niño 3.4 index reached 2.35°C.

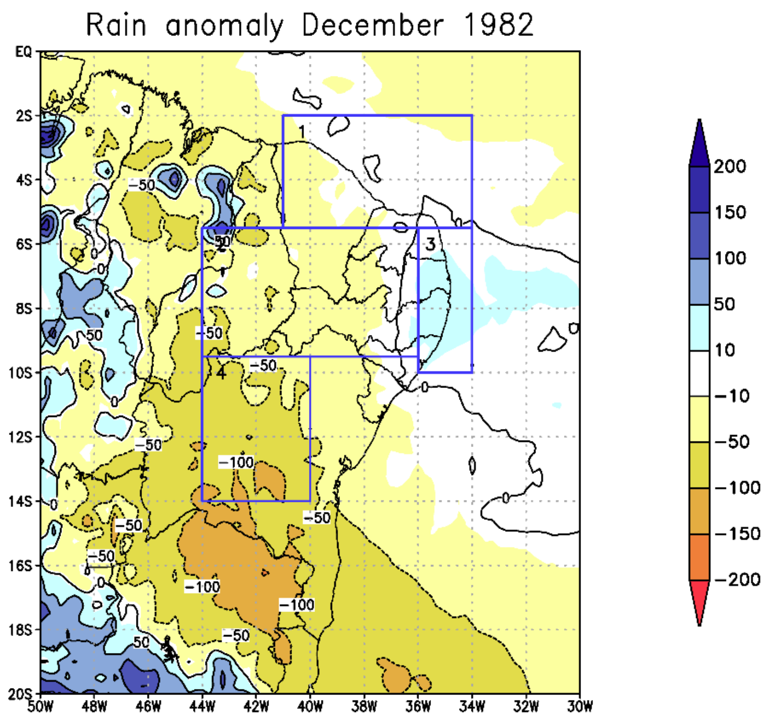

Figure 11. Rain anomalies were observed in Northeast Brazil (NEB) in December 1982, when the warm anomaly of the sea surface temperature (SST) in the Pacific tropical sector, Niño3.4, reached 2.20 °C

Unit: mm per month.

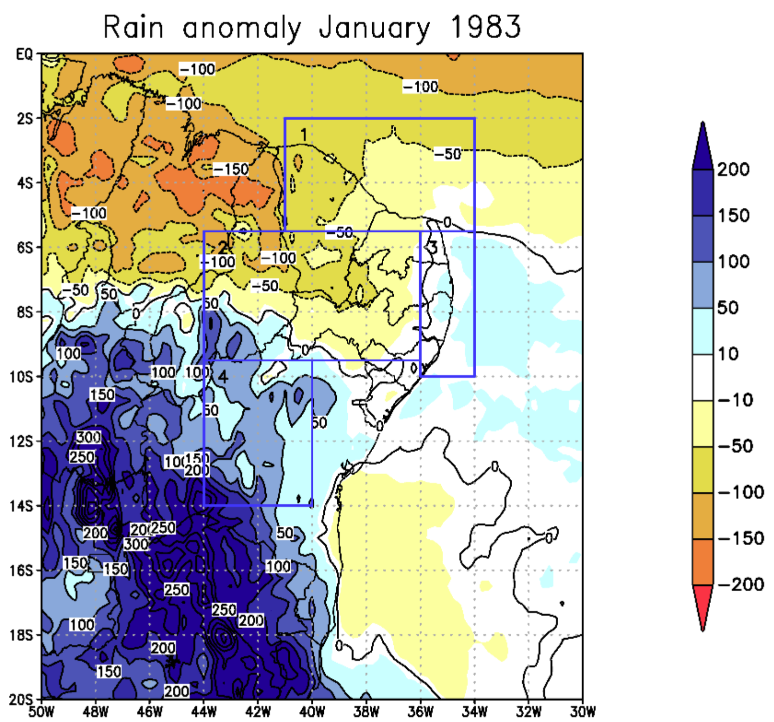

Figure 12. Rain anomalies were observed in Northeast Brazil (NEB) in January 1983, when the warm anomaly of the sea surface temperature (SST) in the Pacific tropical sector, Niño3.4, reached 2.35 °C

Unit: mm per month.

Figures 11 and 12 clearly exemplify what has been called "ENSO diversity" in the literature within the 1982/1983 El Niño event. The monthly precipitation in NEB in December 1982 (Figure 11) represents weak drought in Boxes 1 and 2 and intense drought in Box 4. This drought in Box 4 appears to be connected to an evident suppression of rainfall in the South Atlantic Convergence Zone (SACZ), a typical rainy band that usually occurs at the beginning of summer at subtropical latitudes on the east coast of South America. However, in January 1983 (Figure 12), the drought reached Boxes 1 and 2, extending westward into the eastern sector of Amazonia. Moreover, Box 4, together with the SACZ, was very rainy.

Figure 13 shows the distribution of the vertical gradient $\Delta\theta_e/\Delta p$ during the warm ENSO episode observed in the Pacific from May 1997 to May 1998.

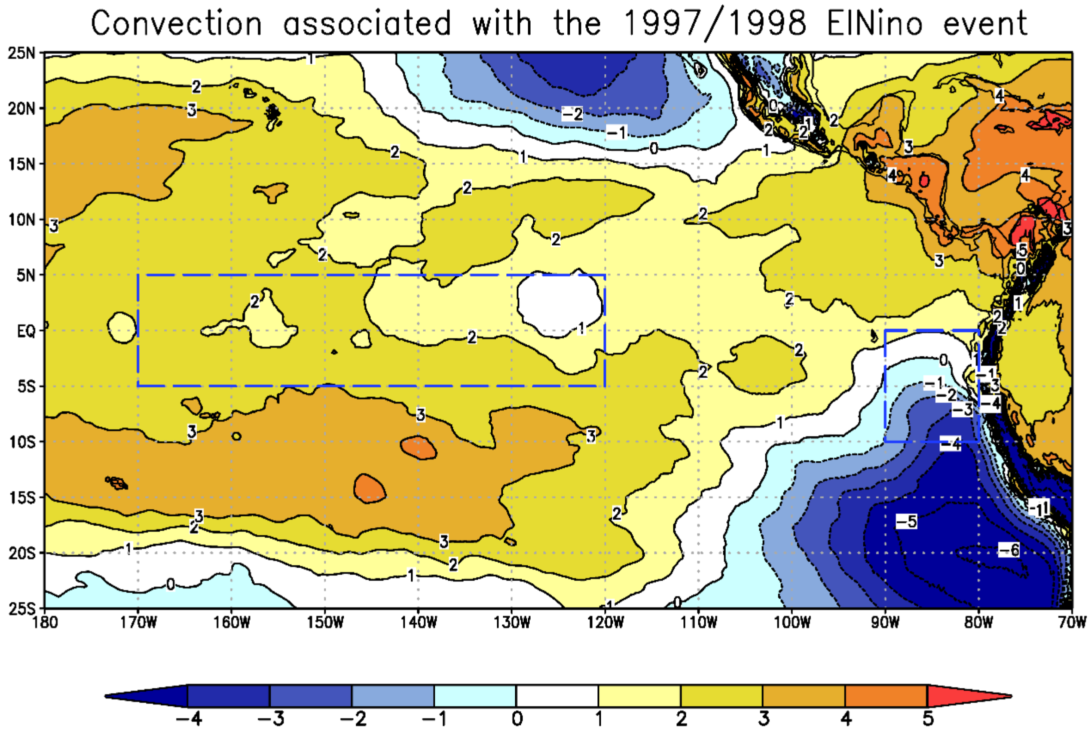

Figure 13. A composite representing the convective response to anomalous warming occurred during the 1997–1998 El Niño event. The Niño1+2 and Niño3.4 sectors are highlighted

Unit: 10^{-4} K/Pa.

Once again, the sector with the most intense convective instability in response to the 1997/1998 El Niño in the Tropical Pacific occurred to the south of the region where the Niño 3.4 index is defined.

Figure 14 shows the convective response, represented by the positive sectors of the vertical gradient $\Delta\theta_e/\Delta p$, to the warming of the waters of the Tropical Pacific during the 18 months of the positive Niño3.4 index in the El Niño event that lasted from November 2014 to April 2016.

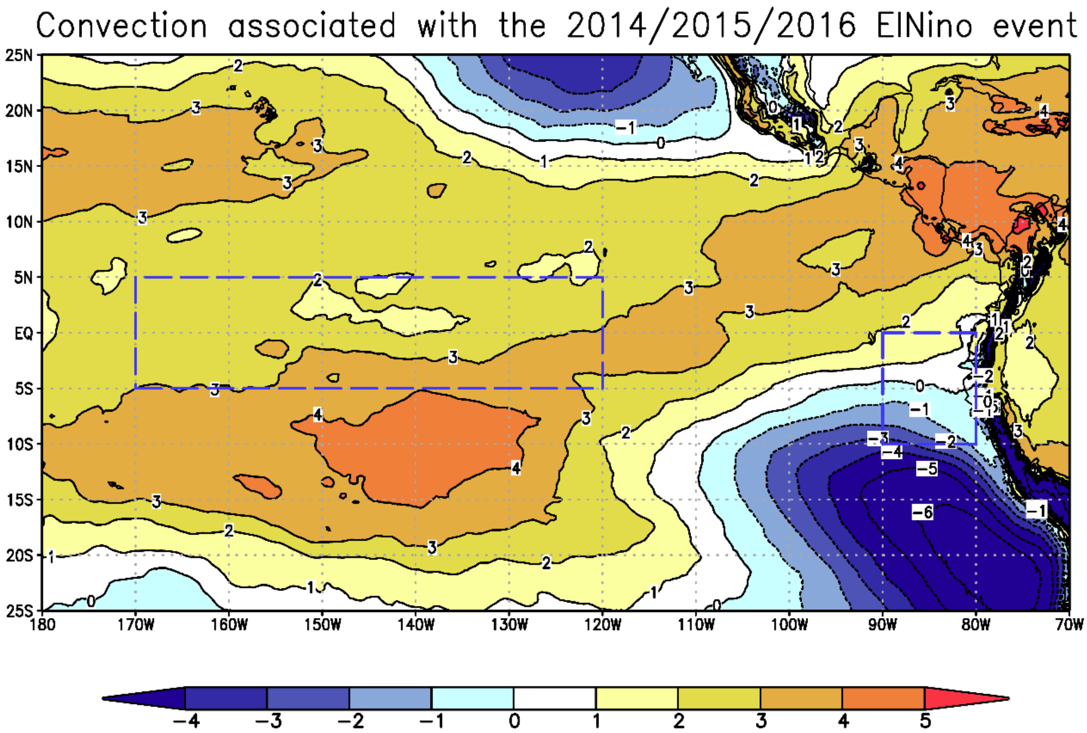

Figure 14. A composite representing the convective response to anomalous warming occurred during the El Niño event of 2014/2015/2016. The Niño1+2 and Niño3.4 sectors are highlighted

Unit: 10^{-4} K/Pa.

The above findings, referring to three notable El Niño episodes, suggest that repositioning of the area with convective activity is more capable of producing the expected remote effects in Northeast Brazil, a little further south of the area recognized as El Niño3.4. The latitudinal limits of this new area would be between 15° S and 5° S, which could be called the Yanai3.4 sector.

4. Conclusion

In recent years, various studies into the remote impacts of El Niño events on climate anomalies observed around the world have come up against a relevant issue, namely, the "diversity of ENSO", i.e., each occurrence of El Niño or La Niña seems to have a different remote response, causing obvious frustration for researchers. This investigation somewhat confirms the lack of confidence in our ability to anticipate the remote effects of ENSO forcings since we have not yet found a persistent correspondence between the intensity of ENSO indices and climate variations in the various target locations of the descending branches of Walker and Hadley cells triggered by El Niño events or their consequences. Similarly, this study was unable to clarify the issue of "ENSO diversity", but instead, we suggest the use of atmospheric indicators, such as the spatial distribution of convective instability in the lower troposphere of the Tropical Pacific, as an alternative approach in the search for evidence of possible remote effects of El Niño events on atmospheric circulation. This research used the approach of Yanai et al. (1973), according to which positive gradients in the equivalent potential temperature in the lower troposphere are robust indicators of the presence of deep convection in response to the warming of surface waters in tropical oceans. The convective responses associated with El Niño events were thus diagnosed.

This approach was based on two steps: (1) the remote connections between El Niño events and the resulting climate anomalies, with a high amount of rain or a lack thereof, are often due to the action of vertical circulation cells of the Walker type and to the eventual occurrence of Hadley-type cells, all of which are driven by cumulonimbus; and (2) the deep cumulus observed in response to the warming of the surface waters of the Tropical Pacific in El Niño events has their positioning controlled not only by the heat and humidity offered by the warmed ocean surface but also by other atmospheric circulation control factors.

There is also a somewhat surprising third pillar: at least in the case of the response to droughts in Northeast Brazil, the statistical analyses carried out here indicate that the different subregions of NEB seem to respond to convective clusters positioned in different subregions in the Tropical Pacific. Therefore, one way of predicting the remote effects of the warm phase of a given ENSO event is to consider the prevailing atmospheric processes over the oceanic processes since global atmospheric dynamics will interfere with the regional convective response in the Tropical Pacific Ocean.

Kayano & Andreoli (2007), for example, showed how ENSO episodes occurring in the Tropical Pacific are affected by the phases of the Pacific Decadal Oscillation, which occurs at the midlatitudes of the North Pacific. Among other conclusions, they showed that the connection between ENSO events and precipitation in South America was considerably stronger when an intense El Niño coincided with the positive phase of the Pacific Decadal Oscillation. Reboita & Santos (2014) described several cases in which rained a lot in NEB, even while El Niño occurred in the Tropical Pacific, although in other periods, there was severe drought.

Therefore, to predict how the global dynamics of the atmosphere will interfere with each warm phase of ENSO, it is certain that the best way to do this is through properly conducted global modeling. Thus, the positioning of deep convection in the tropical Pacific in response to warm surface water anomalies will serve to indicate how the downward movements of vertical cells will remotely affect a particular region, such as Northeast Brazil.

Acknowledgments

The author recognizes the importance of Professor Michio Yanai's approach to determining the role of tropospheric vertical gradients of equivalent potential temperature as indicators of convective instability over tropical oceans with warm surface waters. The author would like to thank Professors Dr. Pedro L. Silva Dias and Dr. Maria F. Silva Dias for demonstrating the importance of thermodynamic diagrams using potential temperatures in tropical studies. The author would also like to thank Dr. Antonietta Capotondi for encouraging the search for new atmospheric indicators related to ENSO. Almost all the figures in this article were prepared using GrADS software (COLA).

References

Betts, A. K., & Silva Dias, M. F. (1979). Unsaturated Downdraft Thermodynamics in Cumulonimbus. *J. Atmos. Sci., 36*, 1061-1071. https://doi.org/10.1175/1520-0469(1979)036<1061:UDTIC>2.0.CO;2

Capotondi, A., Wittenberg, A. T., Newman, M., Lorenzo, E. D., Yu, J. Y., Braconnot, P., … Yeh, S. W. (2015). Understanding ENSO Diversity. *Bull. Amer. Meteor. Soc., 9*, 921-938. https://doi.org/10.1175/BAMS-D-13-00117.1

Chiodi, A. M., & Harrison, D. E. (2015). Global Seasonal Precipitation Anomalies Robustly Associated with El Niño and La Niña Events – An OLR Perspective. *J. Climate, 28*, 6133-6159. https://doi.org/10.1175/JCLI-D-14-00387.1

Hastenrath, S. (2012). Exploring the climate problems of Brazil's Nordeste: a review. *Climate Change, 112*, 243-251. https://doi.org/10.1007/s10584-011-0227-1

Hersbach, H., Bell, B., Berrisford, P., Biavati, G., Horányi, A., Muñoz Sabater, J., … Thépaut, J-N. (2023). *ERA5 monthly averaged data on pressure levels from 1940 to present.* Copernicus Climate Change Service (C3S) Climate Data Store (CDS). https://doi.org/10.24381/cds.6860a573 (Accessed on 15-MAY-2023)

Holton, J. (2004). *An Introduction to Dynamic Meteorology* (4th ed.) Amsterdam: Elsevier Academic Press.

Kayano, M. T., & Andreoli, R. V. (2007). Relations of South American Summer Rainfall Interannual Variations with the Pacific Decadal Oscillation. *Int. J. Climatol., 27*, 531-540. https://doi.org/10.1002/joc.1417

Katz, R. W. (2002). Sir Gilbert Walker and a Connection between El Niño and Statistics. *Statistical Science, 17*, 97-112.

Kousky, V. E. (1980). Diurnal rainfall variation in northeast Brazil. *Mon. Wea. Rev., 108*, 488-498. https://doi.org/10.1175/1520-0493(1980)108<0488:DRVINB>2.0.CO;2

Reboita, M. S., & Santos, I. A. (2014). Influence of some Teleconnection Patterns on Precipitation in North and Northeast Brazil (in Portuguese). *Revista Brasileira de Climatologia, 15*, 28-48. https://doi.org/10.5380/abclima.v15i0.37686

Silva Dias, P. L., Schubert, W. H., & DeMaria, M. (1983). Large-Scale Response of the Atmosphere to Transient Convection. *J. Atmos. Sci., 40*, 2689-2707. https://doi.org/10.1175/1520-0469(1983)040<2689:LSROTT>2.0.CO;2

Walker, G. T., & Bliss, E. W. (1932). World Weather VI. *Mem. Roy. Meteor. Soc., 4*, 53-84.

Yanai, M., Esbensen, S., & Chu, J. (1973). Determination of Bulk Properties of Tropical Cloud Clusters from Large-Scale Heat and Moisture Budgets. *J. Atmos. Sci., 30*, 611-627.